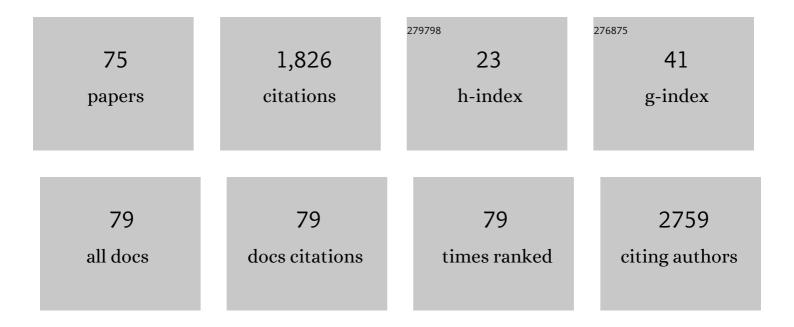
List of Publications by Year in descending order

Source: https://exaly.com/author-pdf/2012840/publications.pdf Version: 2024-02-01



DONG-KYUN SEO

#	Article	IF	CITATIONS
1	Heterogeneous catalysts for biomass-derived alcohols and acid conversion. , 2022, , 297-326.		0
2	Ketonic decarboxylation and esterification of propionic acid over beta zeolites. Microporous and Mesoporous Materials, 2021, 310, 110628.	4.4	8
3	Laâ€Hâ€zeolites: efficient catalysts for acetic acid ketonic decarboxylation and esterification. Journal of Chemical Technology and Biotechnology, 2021, 96, 2022-2032.	3.2	1
4	Photoelectrochemical Water Oxidation by Cobalt Cytochrome C Integrated-ATO Photoanode. Catalysts, 2021, 11, 626.	3.5	2
5	Interfacing Photosystem I Reaction Centers with a Porous Antimony-Doped Tin Oxide Electrode to Perform Light-Driven Redox Chemistry. ACS Applied Electronic Materials, 2021, 3, 2087-2096.	4.3	7
6	Role of oxygen vacancies and Mn4+/Mn3+ ratio in oxidation and dry reforming over cobalt-manganese spinel oxides. Molecular Catalysis, 2020, 483, 110704.	2.0	14
7	High-surface area mesoporous carbons from gel templating and inorganic-organic hybrid gel formation. Journal of Solid State Chemistry, 2020, 281, 121040.	2.9	4
8	Effects of Wax-Impregnated Nanozeolites on Bitumen's Thermomechanical Properties. ACS Sustainable Chemistry and Engineering, 2020, 8, 15299-15309.	6.7	7
9	Selective oxidation of <i>n</i> -buthanol to butyraldehyde over MnCo ₂ O ₄ spinel oxides. RSC Advances, 2020, 10, 25125-25135.	3.6	7
10	Synthesized Geopolymers Adsorb Bacterial Proteins, Toxins, and Cells. Frontiers in Bioengineering and Biotechnology, 2020, 8, 527.	4.1	10
11	Polyamide thin-film nanocomposite membranes with graphene oxide nanosheets: Balancing membrane performance and fouling propensity. Desalination, 2019, 451, 139-147.	8.2	85
12	Exploratory Synthesis of Low-Silica Nanozeolites through Geopolymer Chemistry. Crystal Growth and Design, 2019, 19, 1167-1171.	3.0	12
13	Self-emitting blue and red EuOX (X = F, Cl, Br, I) materials: band structure, charge transfer energy, and emission energy. Physical Chemistry Chemical Physics, 2019, 21, 1737-1749.	2.8	22
14	Molybdenum Dopped Copper Ferrites as Active Catalysts for Alcohols Oxidative Coupling. Materials, 2019, 12, 1871.	2.9	7
15	The Oxidative Coupling Between Methanol and Ethanol Over Copper Ferrites with Vanadium. Catalysis Letters, 2019, 149, 2043-2052.	2.6	0
16	Steam reforming of toluene as model of tar compound over Mo catalysts derived from hydrotalcites. Journal of Saudi Chemical Society, 2019, 23, 916-924.	5.2	6
17	Evaluation and optimization of VPSA processes with nanostructured zeolite NaX for post-combustion CO2 capture. Chemical Engineering Journal, 2019, 371, 693-705.	12.7	69
18	Interfacing Photosystem I Reaction Centers with a Porous Antimony-Doped Tin Oxide Electrode to Perform Light Driven Redox Chemistry. Biophysical Journal, 2019, 116, 443a.	0.5	1

#	Article	IF	CITATIONS
19	Superior ion release properties and antibacterial efficacy of nanostructured zeolites ion-exchanged with zinc, copper, and iron. RSC Advances, 2018, 8, 37949-37957.	3.6	32
20	Thickness-Dependent Bioelectrochemical and Energy Applications of Thickness-Controlled Meso-Macroporous Antimony-Doped Tin Oxide. Coatings, 2018, 8, 128.	2.6	1
21	New hydrogen titanium phosphate sulfate electrodes for Li-ion and Na-ion batteries. Journal of Power Sources, 2017, 343, 197-206.	7.8	18
22	A highly stable and scalable photosynthetic reaction center–graphene hybrid electrode system for biomimetic solar energy transduction. Journal of Materials Chemistry A, 2017, 5, 6038-6041.	10.3	13
23	Tracking Single DNA Nanodevices in Hierarchically Meso-Macroporous Antimony-Doped Tin Oxide Demonstrates Finite Confinement. Langmuir, 2017, 33, 6410-6418.	3.5	3
24	Silver-Ion-Exchanged Nanostructured Zeolite X as Antibacterial Agent with Superior Ion Release Kinetics and Efficacy against Methicillin-Resistant <i>Staphylococcus aureus</i> . ACS Applied Materials & Interfaces, 2017, 9, 39271-39282.	8.0	36
25	Enhancing Photocurrent Generation in Photosynthetic Reaction Centerâ€Based Photoelectrochemical Cells with Biomimetic DNA Antenna. ChemSusChem, 2017, 10, 4457-4460.	6.8	5
26	Hydrotalcites with vanadium, effective catalysts for steam reforming of toluene. International Journal of Hydrogen Energy, 2017, 42, 21732-21740.	7.1	13
27	Template-free synthesis and structural evolution of discrete hydroxycancrinite zeolite nanorods from high-concentration hydrogels. Nanoscale, 2017, 9, 18804-18811.	5.6	9
28	Highly Selective Solid Acid Catalyst H1â^'xTi2(PO4)3â^'x(SO4)x for Non-Oxidative Dehydrogenation of Methanol and Ethanol. Catalysts, 2017, 7, 95.	3.5	11
29	Coarsening and Spinodal Decomposition of Zeolite Linde Type A Precursor Gels Aged at Low Temperatures. Crystal Growth and Design, 2016, 16, 3224-3230.	3.0	11
30	Effect of Mo/Ce ratio in Mo–Ce–Al catalysts on the hydrogen production by steam reforming of glycerol. Catalysis Science and Technology, 2016, 6, 7902-7912.	4.1	8
31	Equipment-Free Deposition of Graphene-Based Molybdenum Oxide Nanohybrid Langmuir–Blodgett Films for Flexible Electrochromic Panel Application. ACS Applied Materials & Interfaces, 2016, 8, 21539-21544.	8.0	22
32	Photocurrent Generation by Photosynthetic Purple Bacterial Reaction Centers Interfaced with a Porous Antimony-Doped Tin Oxide (ATO) Electrode. ACS Applied Materials & Interfaces, 2016, 8, 25104-25110.	8.0	15
33	Unusual Changes in Electronic Band-Edge Energies of the Nanostructured Transparent n-Type Semiconductor Zr-Doped Anatase TiO ₂ (Ti _{1â€"<i>x</i>} Zr _{<i>x</i>} O ₂ ; <i>x</i> < 0.3). Inorganic Chemistry, 2016, 55, 6574-6585.	4.0	14
34	Hydrogen production from glycerol steam reforming over molybdena–alumina catalysts. Catalysis Communications, 2016, 77, 83-88.	3.3	23
35	Accessing alkali-free NASICON-type compounds through mixed oxoanion sol–gel chemistry: Hydrogen titanium phosphate sulfate, H1â^Ti2(PO4)3â^ (SO4) (x=0.5–1). Journal of Solid State Chemistry, 2016, 242, 116-125.	2.9	9
36	Remarkable flux effect of Li-codoping on highly enhanced luminescence of orthosilicate Ba ₂ SiO ₄ :Eu ²⁺ phosphors for NUV-LEDs: autonomous impurity purification by eutectic Li ₂ CO ₃ melts. RSC Advances, 2015, 5, 105339-105346.	3.6	13

#	Article	IF	CITATIONS
37	Nanoporous Delafossite CuAlO ₂ from Inorganic/Polymer Double Gels: A Desirable High-Surface-Area p-Type Transparent Electrode Material. Inorganic Chemistry, 2015, 54, 1100-1108.	4.0	20
38	Calcium-modified hierarchically porous aluminosilicate geopolymer as a highly efficient regenerable catalyst for biodiesel production. RSC Advances, 2015, 5, 65454-65461.	3.6	67
39	Blue-silica by Eu ²⁺ -activator occupied in interstitial sites. RSC Advances, 2015, 5, 74790-74801.	3.6	70
40	Iron oxide-modified nanoporous geopolymers for arsenic removal from ground water. Resource-efficient Technologies, 2015, 1, 19-27.	0.1	27
41	Geopolymer with Hierarchically Meso″Macroporous Structures from Reactive Emulsion Templating. Journal of the American Ceramic Society, 2014, 97, 70-73.	3.8	71
42	Concomitant Thionation and Reduction of Graphene Oxide Through Solid/Gas Metathetical Sulfidation Reactions at High Temperatures. Phosphorus, Sulfur and Silicon and the Related Elements, 2014, 189, 721-737.	1.6	11
43	Structural analysis of highly porous γ-Al2O3. Journal of Solid State Chemistry, 2014, 217, 1-8.	2.9	223
44	Preparation and electrochemical properties of nanoporous transparent antimony-doped tin oxide (ATO) coatings. Journal of Materials Chemistry A, 2013, 1, 699-706.	10.3	33
45	Spectroelectrochemistry of cytochrome c and azurin immobilized in nanoporous antimony-doped tin oxide. Chemical Communications, 2011, 47, 12367.	4.1	34
46	One-pot synthesis of highly mesoporous antimony-doped tin oxide from interpenetrating inorganic/organic networks. Journal of Materials Chemistry, 2011, 21, 13232.	6.7	39
47	Size-Selective Incorporation of DNA Nanocages into Nanoporous Antimony-Doped Tin Oxide Materials. ACS Nano, 2011, 5, 6060-6068.	14.6	18
48	Preparation of Nanoporous MgAl2O4 by Combined Utilization of Sol-Gel Process and Combustion of Biorenewable Oil. Materials Research Society Symposia Proceedings, 2011, 1306, 1.	0.1	0
49	A synthetic strategy of quantum dot-bioconjugate. , 2010, , .		0
50	Preparation of highly porous Î ³ -alumina via combustion of biorenewable oil. Journal of Materials Chemistry, 2010, 20, 5923.	6.7	12
51	Optically tandem thin film solar cells. , 2009, , .		0
52	Preparation of photostable quantum dot-polystyrene microbeads through covalent organosilane coupling of CdSe@Zns quantum dots. Journal of Materials Science, 2009, 44, 816-820.	3.7	14
53	Nature of Stoner condition for metallic ferromagnetism. Journal of Computational Chemistry, 2008, 29, 2172-2176.	3.3	12
54	Report from the third workshop on future directions of solid-state chemistry: The status of solid-state chemistry and its impact in the physical sciences. Progress in Solid State Chemistry, 2008, 36, 1-133.	7.2	58

#	Article	IF	CITATIONS
55	Orbital Interpretation of Kinetic Energy Density and a Direct Space Comparison of Chemical Bonding in Tetrahedral Network Solids. Journal of Physical Chemistry A, 2008, 112, 7705-7716.	2.5	4
56	Two-Dimensional Superdegeneracy and Structureâ^'Magnetism Correlations in Strong Ferromagnet, Mn ₂ Ga ₅ . Journal of the American Chemical Society, 2008, 130, 1384-1391.	13.7	19
57	Density functional perturbational orbital theory of spin polarization in electronic systems. II. Transition metal dimer complexes. Journal of Chemical Physics, 2007, 127, 184103.	3.0	6
58	A Facile One-Step in situ Functionalization of Quantum Dots with Preserved Photoluminescence for Bioconjugation. Journal of the American Chemical Society, 2007, 129, 6380-6381.	13.7	105
59	Self-interaction correction in the <mml:math <br="" xmlns:mml="http://www.w3.org/1998/Math/MathML">display="inline"><mml:mrow><mml:mi>LDA</mml:mi><mml:mo>+</mml:mo><mml:mi mathvariant="normal">U</mml:mi </mml:mrow></mml:math> method. Physical Review B, 2007, 76, .	3.2	18
60	Synthesis of Deep-Red-Emitting CdSe Quantum Dots and General Non-Inverse-Square Behavior of Quantum Confinement in CdSe Quantum Dots. Chemistry of Materials, 2006, 18, 5764-5767.	6.7	59
61	Electon-Precise/Deficient La5-xCaxGe4 (3.4 ≤ ≤3.8) and Ce5-xCaxGe4 (3.0 ≤ ≤3.3): Probing Low-Vale Electron Concentrations in Metal-Rich Gd5Si4-Type Germanides ChemInform, 2006, 37, no.	ence 0.0	1
62	Density functional perturbational orbital theory of spin polarization in electronic systems. I. Formalism. Journal of Chemical Physics, 2006, 125, 154105.	3.0	11
63	Preparation of Large Transparent Silica Monoliths with Embedded Photoluminescent CdSe@ZnS Core/Shell Quantum Dots. Chemistry of Materials, 2005, 17, 4762-4764.	6.7	78
64	Observation of Unusual Hysteretic Magnetic Properties of the Rare Earth Intermetallic Compound PrMnSi2: Magnetic Susceptibility, Magnetization, Heat Capacity, and Electronic Band Structure Studies ChemInform, 2005, 36, no.	0.0	0
65	Electron-Precise/Deficient La5-xCaxGe4(3.4 ≤≤3.8) and Ce5-xCaxGe4(3.0 ≤≤3.3): Probing Low-Valer Electron Concentrations in Metal-Rich Gd5Si4-type Germanides. Journal of the American Chemical Society, 2005, 127, 15682-15683.	nce 13.7	46
66	Large Negative Magnetoresistance of the Rare-Earth Transition-Metal Intermetallic Compound PrMnSi2. Chemistry of Materials, 2005, 17, 6338-6341.	6.7	5
67	Observation of Unusual Hysteretic Magnetic Properties of the Rare Earth Intermetallic Compound PrMnSi2:  Magnetic Susceptibility, Magnetization, Heat Capacity, and Electronic Band Structure Studies. Chemistry of Materials, 2005, 17, 3711-3716.	6.7	3
68	Low-temperature synthetic method for size-controlled CdSe nanocrystals: utilization of boron selenide. Chemical Communications, 2004, , 2298.	4.1	21
69	New Solidâ^'Gas Metathetical Synthesis of Binary Metal Polysulfides and Sulfides at Intermediate Temperatures:Â Utilization of Boron Sulfides. Journal of the American Chemical Society, 2004, 126, 4676-4681.	13.7	47
70	Metathetical Conversion of Nd2O3Nanoparticles into NdS2Polysulfide Nanoparticles at Low Temperatures Using Boron Sulfides. Inorganic Chemistry, 2003, 42, 5798-5800.	4.0	24
71	Synthesis, Structure, and Bonding of BaTl3:  An Unusual Competition between Cluster and Classical Bonding in the Thallium Layers. Journal of the American Chemical Society, 2002, 124, 415-420.	13.7	16
72	Synthesis, Structure, and Bonding of Open-Shell Sr3In5:Â An Unusual Electron Deficiency in an Indium Network, beyond the Zintl Boundary. Journal of the American Chemical Society, 2001, 123, 4512-4518.	13.7	37

#	Article	IF	CITATIONS
73	CHEMISTRY: Aromatic Metal Clusters. Science, 2001, 291, 841-842.	12.6	43
74	Synthesis, Structure, and Bonding of Hypoelectronic SrIn4:Â Direct Example of a Dominant Size Effect in Structure Selection. Journal of the American Chemical Society, 2000, 122, 9621-9627.	13.7	54
75	Understanding Structure-forming Factors and Theory-guided Exploration of Structure–Property Relationships in Intermetallics. , 0, , 183-193.		1